

Support information for

Rationally molecular design: functional quinoline derivatives for PA detection, gaseous acid/base switching and anion-controlled

Yuqing Ma,^a Yuyang Zhang,^a Lin Kong^a, Jiaxiang Yang*^a

^a*College of Chemistry & Chemical Engineering, Anhui University, Anhui Province
Key Laboratory of chemistry for Inorganic/Organic Hybrid Functional Materials,
Hefei 230601, P. R. China. jxyang@ahu.edu.cn*

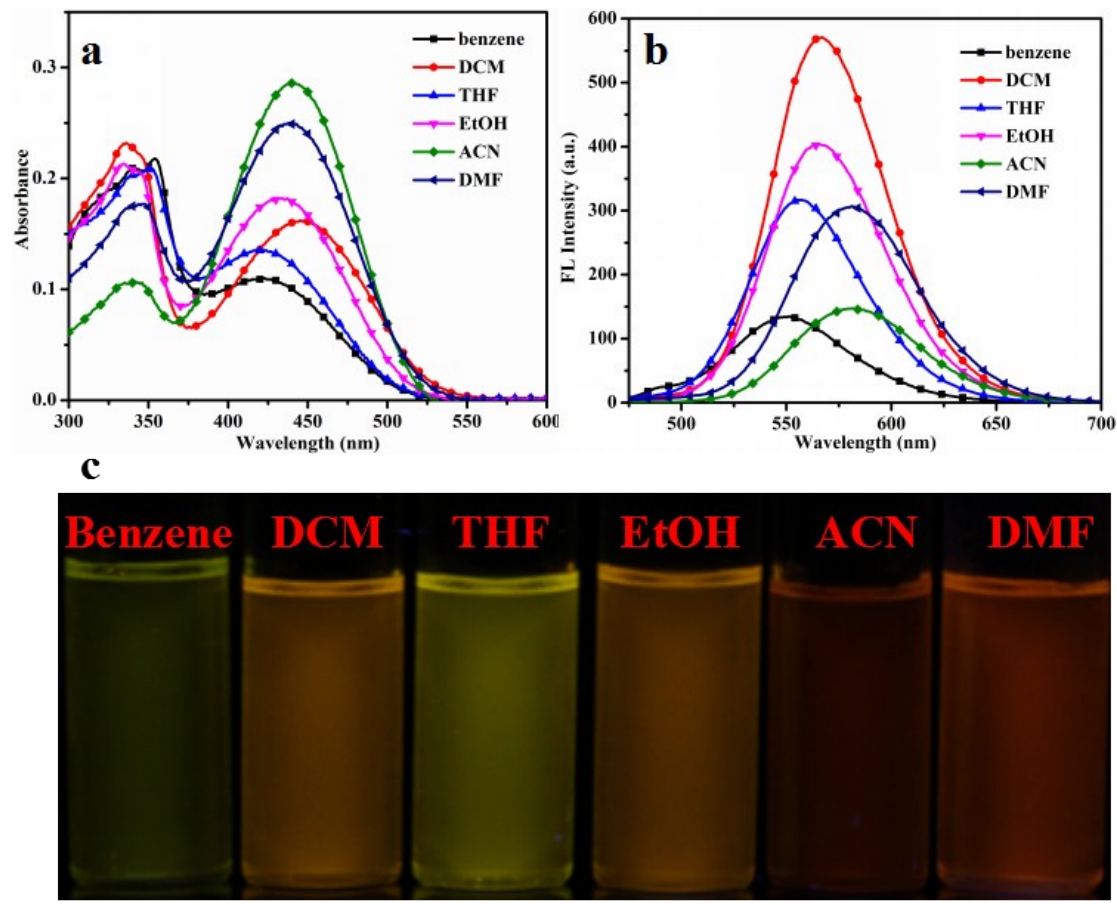


Fig. S1 (a) The UV-Vis spectra; (b) fluorescence spectra of **G2** in different solvents and (c) Photographs of compound **G2** dispersed in different solvents

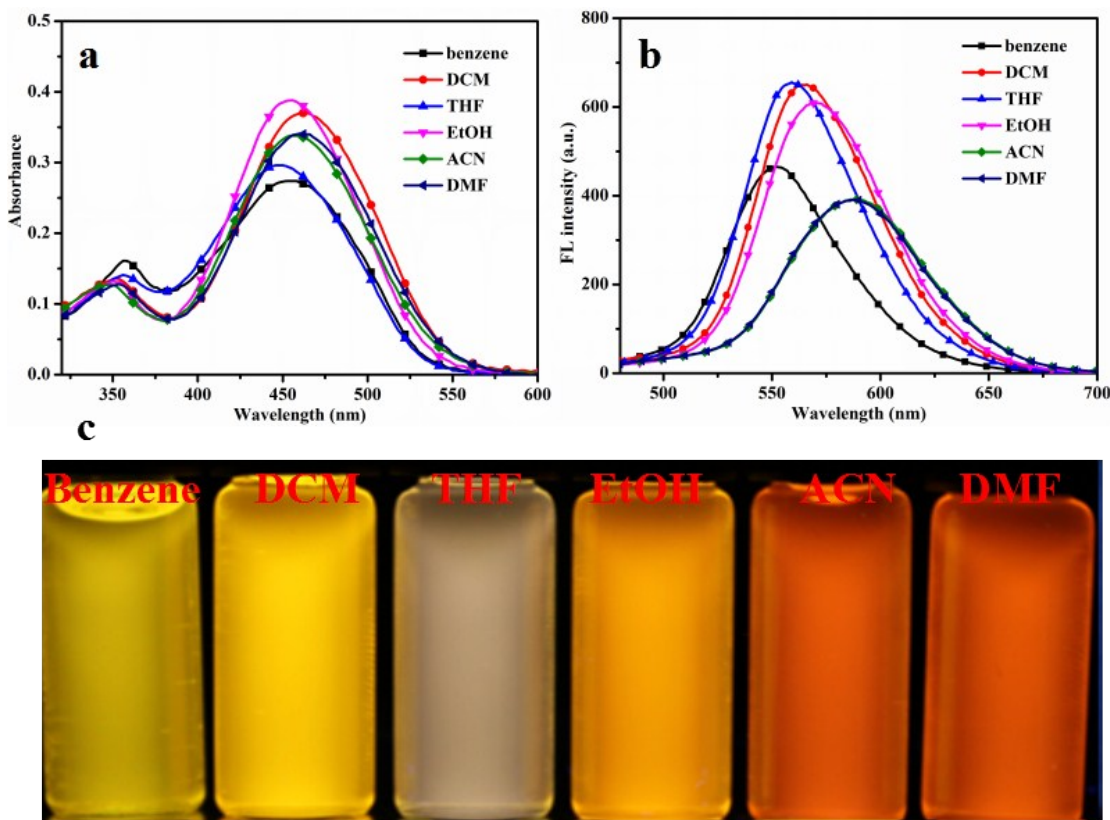


Fig. S2 (a) The UV-vis spectra; (b) fluorescence spectra of **G3** in different solvents and (c) Photographs of compound **G3** dispersed in different solvents

Table S1 The UV-vis absorption data of **G1-G3** in different solvents

	Benzene	DCM	THF	EtOH	ACN	DMF
G₁	$\lambda_{\text{max}}(\text{nm})$	421	445	420	428	438
	$\epsilon_{\text{max}}(10^4)$	1.10	1.62	1.35	1.82	2.86
G₂	$\lambda_{\text{max}}(\text{nm})$	421	446	419	434	430
	$\epsilon_{\text{max}}(10^4)$	0.72	1.30	0.84	1.34	1.51

G₃	$\lambda_{\text{max}}(\text{nm})$	455	460	447	452	457	457
	$\epsilon_{\text{max}}(10^4)$	2.74	3.70	2.96	3.88	3.38	3.41

Table S2 The fluorescent data of **G1-G3** in different solvents

		Benzene	DCM	THF	EtOH	ACN	DMF
G₁	$\lambda_{\text{max}}(\text{nm})$	553	585	558	581	592	591
G₂	$\lambda_{\text{max}}(\text{nm})$	551	567	557	565	582	581
G₃	$\lambda_{\text{max}}(\text{nm})$	552	564	559	570	586	588

Table S3 The relative data of **G1-G3** in different solvents

	Benzene	DCM	THF	EtOH	ACN	DMF
ϵ	2.28	9.10	7.58	25.70	37.50	36.71
n	1.5011	1.4244	1.407	1.3614	1.3441	1.4282
Δf	0.0029	0.2184	0.2671	0.2901	0.3054	0.2752

Table S4 The Stokes' shift of **G1-G3** in different solvents

		Benzene	DCM	THF	EtOH	ACN	DMF
G₁	$\lambda_{\text{abs}}/\text{nm}$	428	448	420	430	428	428
	$\lambda_{\text{em}}/\text{nm}$	553	585	558	581	592	591
	$\Delta\nu/\text{cm}^{-1}$	5281	5227	5888	6044	6472	6444
G₂	$\lambda_{\text{abs}}/\text{nm}$	423	446	421	433	440	438
	$\lambda_{\text{em}}/\text{nm}$	551	567	557	565	582	581
	$\Delta\nu/\text{cm}^{-1}$	5492	4785	5800	5396	5545	5619
G₃	$\lambda_{\text{abs}}/\text{nm}$	454	462	448	454	456	460
	$\lambda_{\text{em}}/\text{nm}$	552	564	559	570	586	588
	$\Delta\nu/\text{cm}^{-1}$	3910	3910	4432	4482	4864	4732

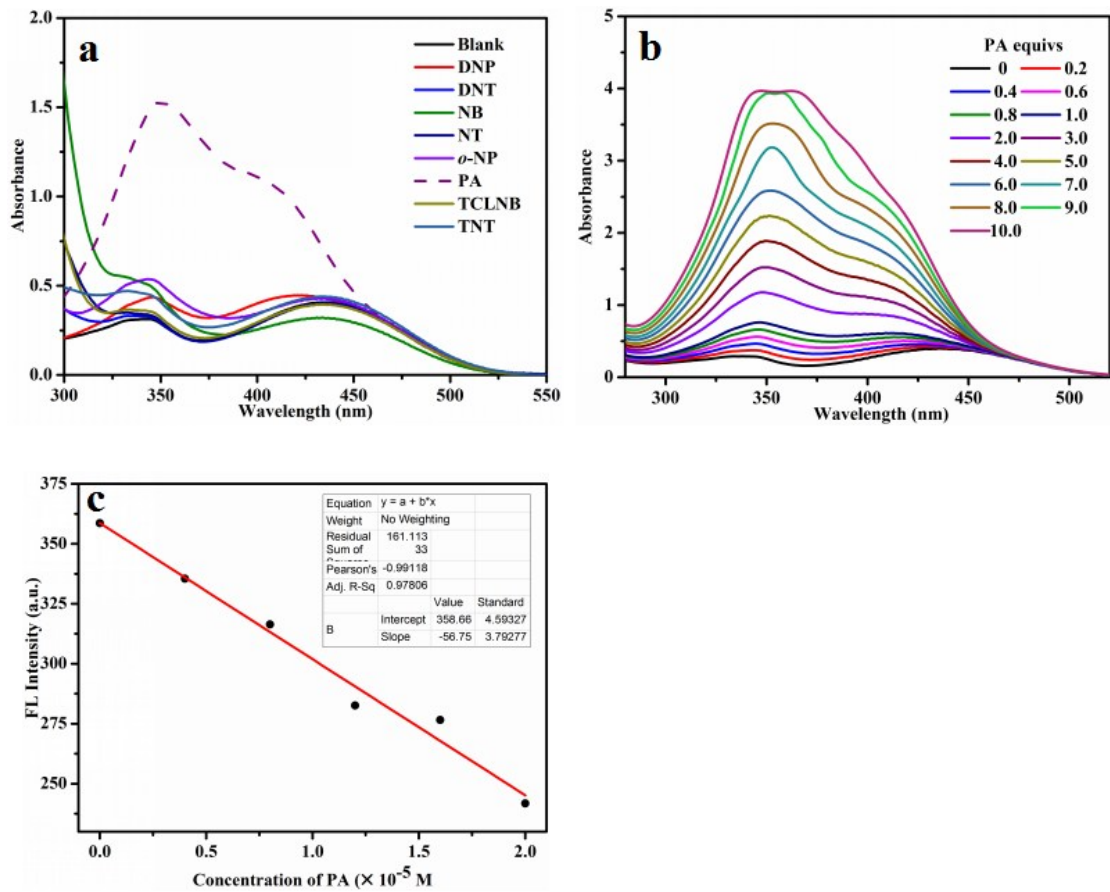


Fig. S3 (a) UV-vis absorption spectra of different nitroaromatic compounds; (b) UV-vis absorption spectra of different concentrations of PA in **G1** solution; (c) The linear relationship between the fluorescence intensity and the PA concentration in **G1** solution

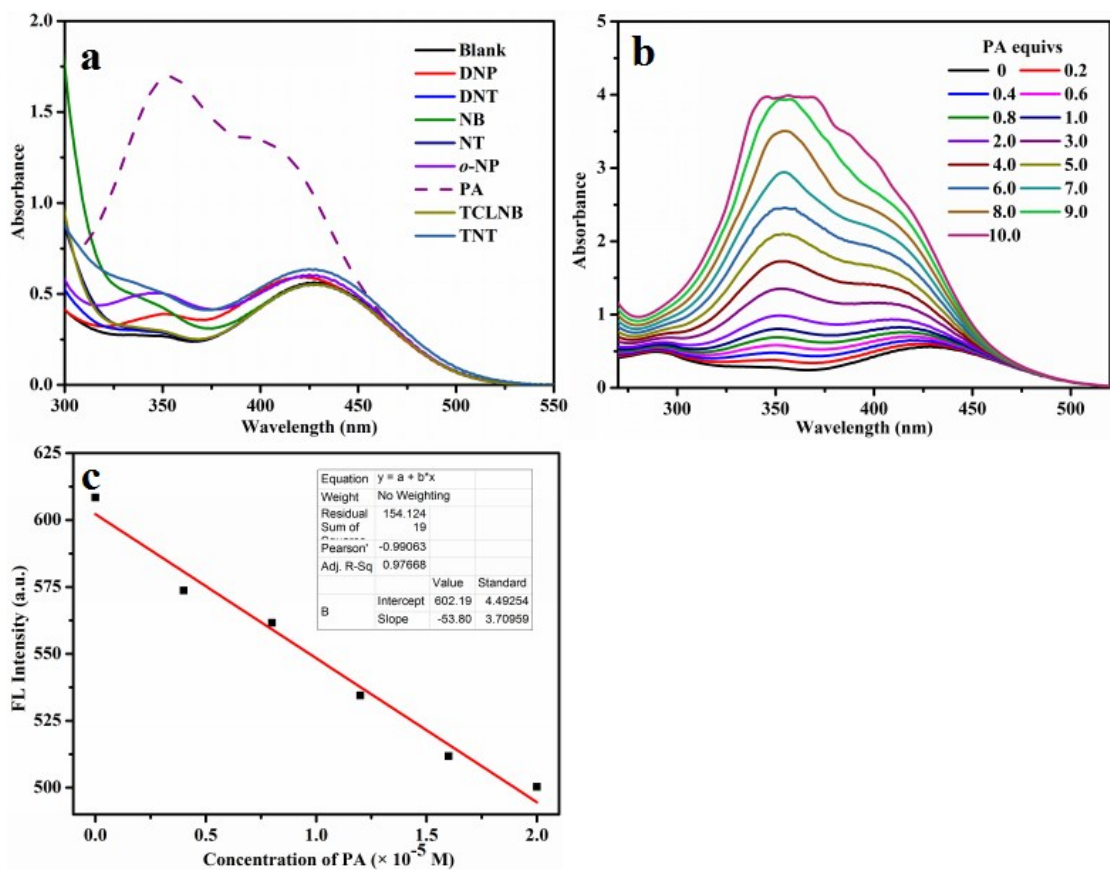


Fig. S4 (a) UV-vis absorption spectra of different nitroaromatic compounds; (b) UV-vis absorption spectra of different concentrations of PA in **G2** solution; (c) The linear relationship between the fluorescence intensity and the PA concentration in **G2** solution

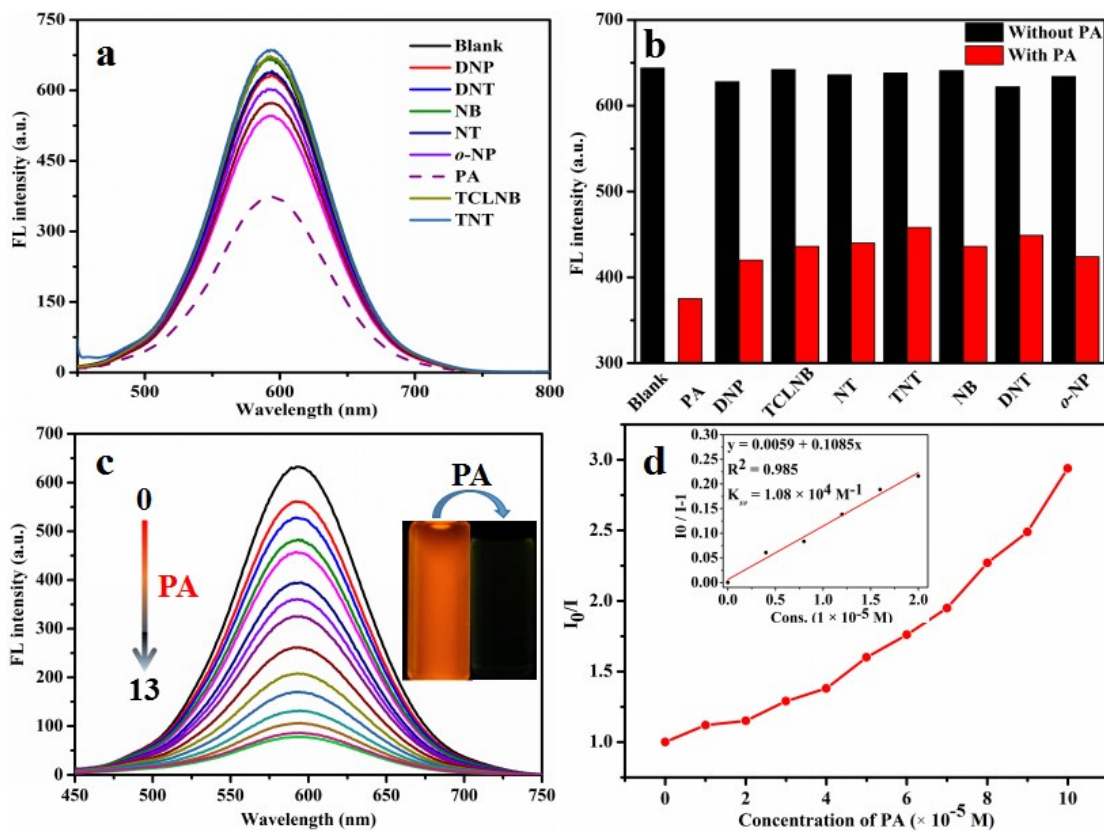


Fig. S5 (a) FL spectra obtained for different analytes (100 ppm); (b) Quenching percentage of compound **G2** (10 mM) with analytes (200 ppm) in CH₃OH/water (v/v = 90 : 10) mixtures before (black) and after (red) the addition of 100 ppm PA; (c) FL spectra of **G2** in CH₃OH/water (v/v = 90 : 10) containing different amounts of PA; (d) Corresponding Stern-Volmer plot of PA. Inset: Stern-Volmer plot obtained at lower concentration of PA

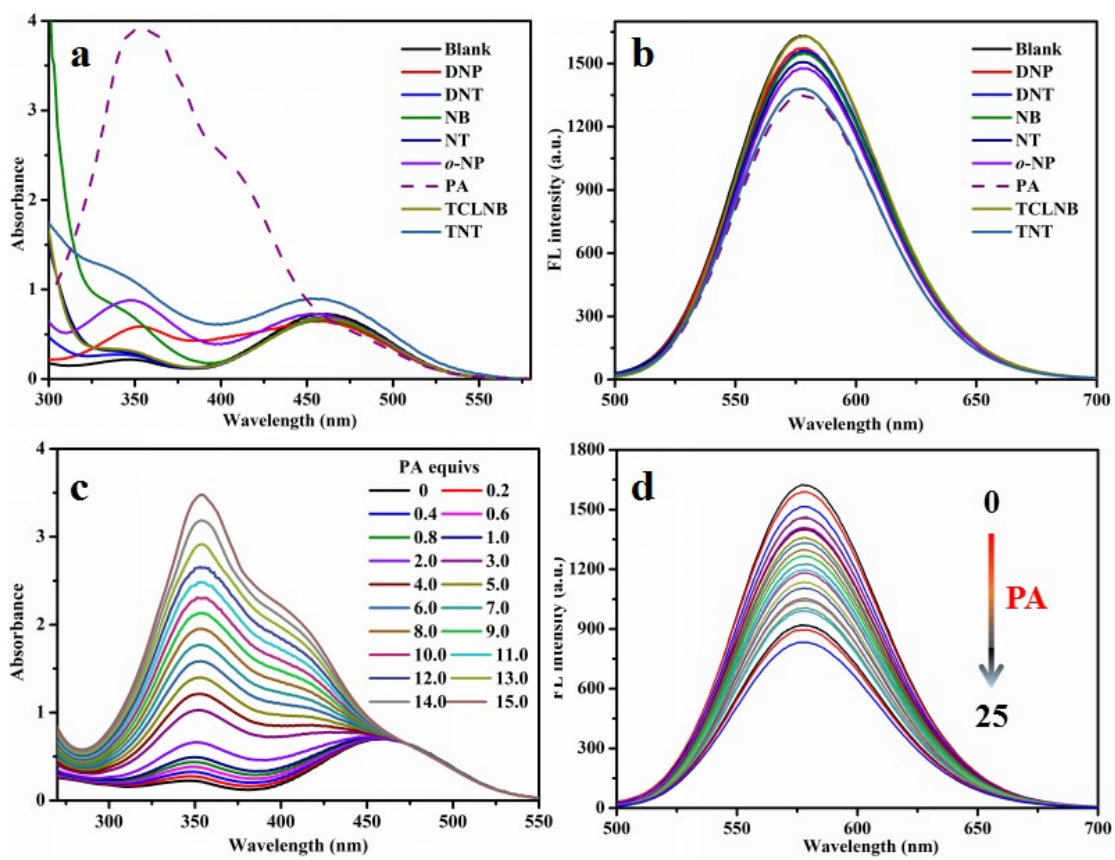
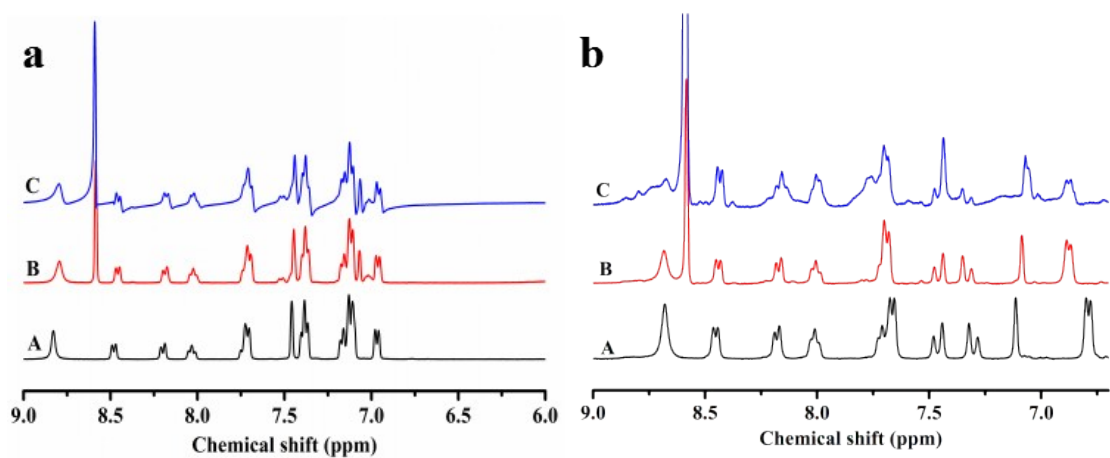
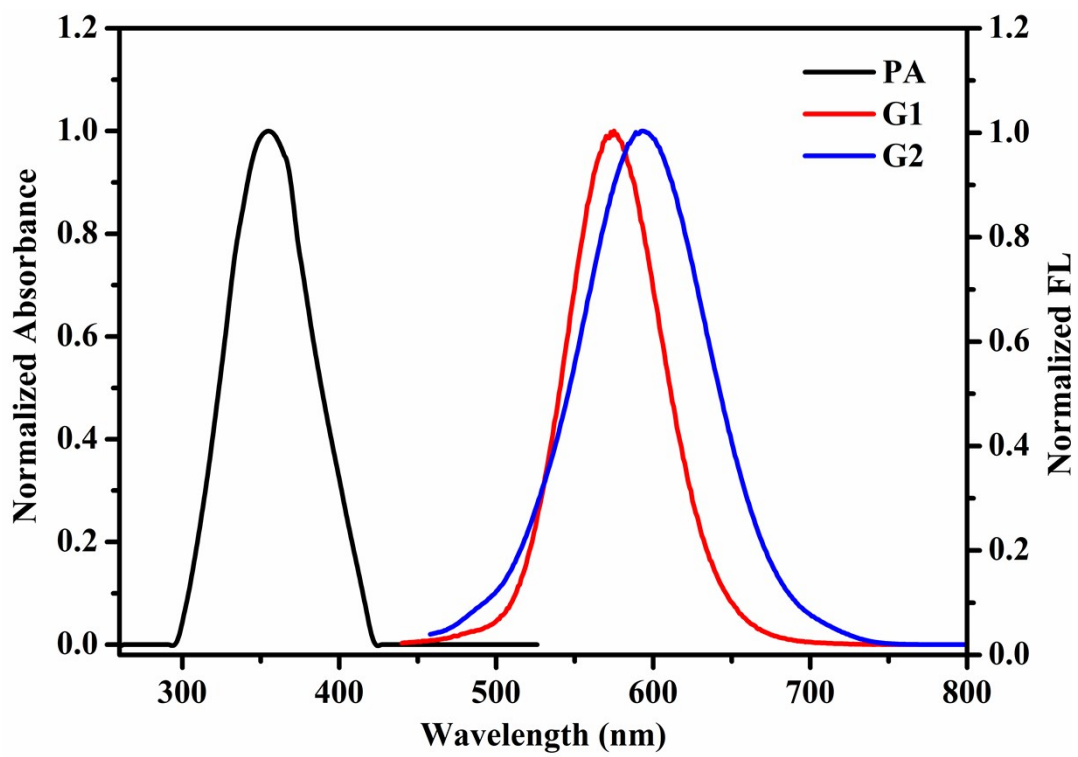


Fig. S6 (a) UV-vis absorption spectra of different nitroaromatic compounds; (B) FL spectra obtained for different analytes (300 ppm); (C) UV-vis absorption spectra of different concentrations of PA in **G3** solution; (D) FL spectra of **G3** in CH₃OH/water (v/v = 90 : 10) containing different amounts of PA



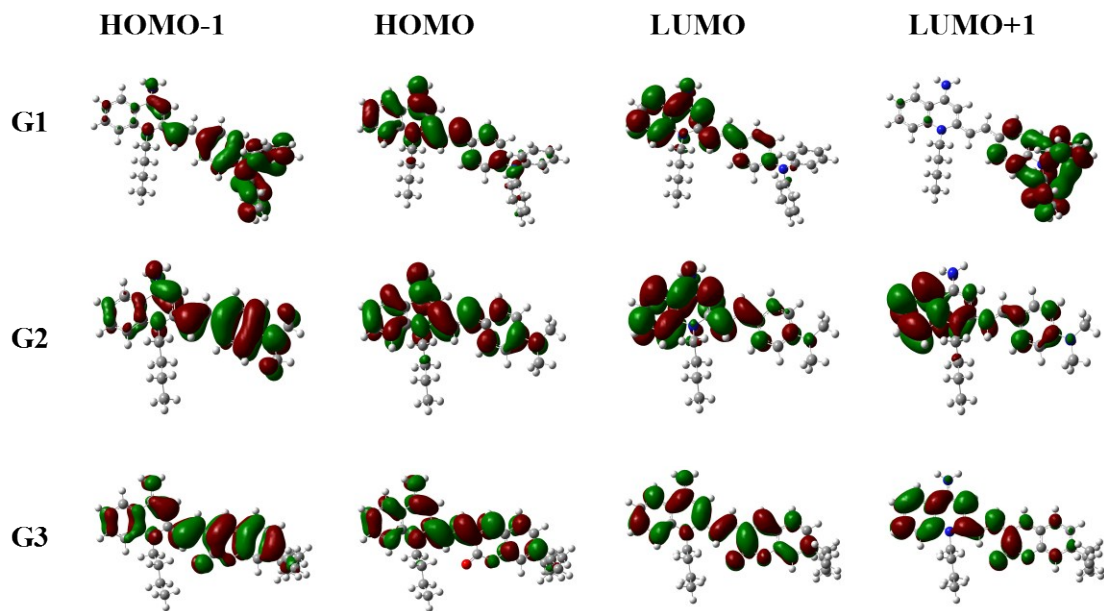


Fig. S9 Frontier orbitals of compounds **G1**, **G2** and **G3**

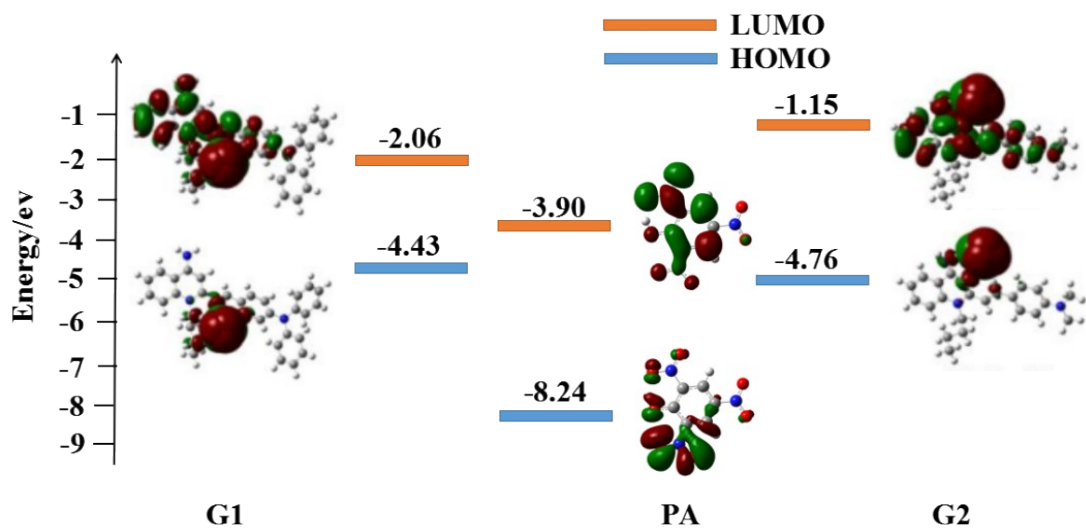


Fig. S10 HOMO and LUMO energy-level diagram of **G1**, **G2** and **PA**

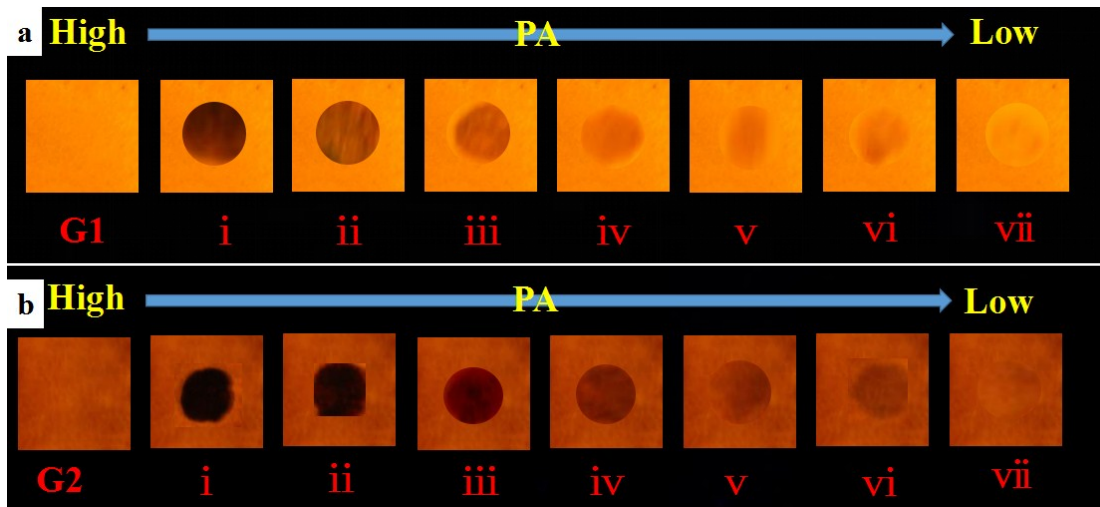


Fig. S11 Photographs of fluorescence quenching of **G1** (a) and **G2** (b) for detecting different concentrations of PA under 365 nm UV light. From left to right: blank, 5.0×10^{-2} , 1.0×10^{-2} , 5.0×10^{-3} , 1.0×10^{-3} , 5.0×10^{-4} , 1.0×10^{-4} , 5.0×10^{-5}

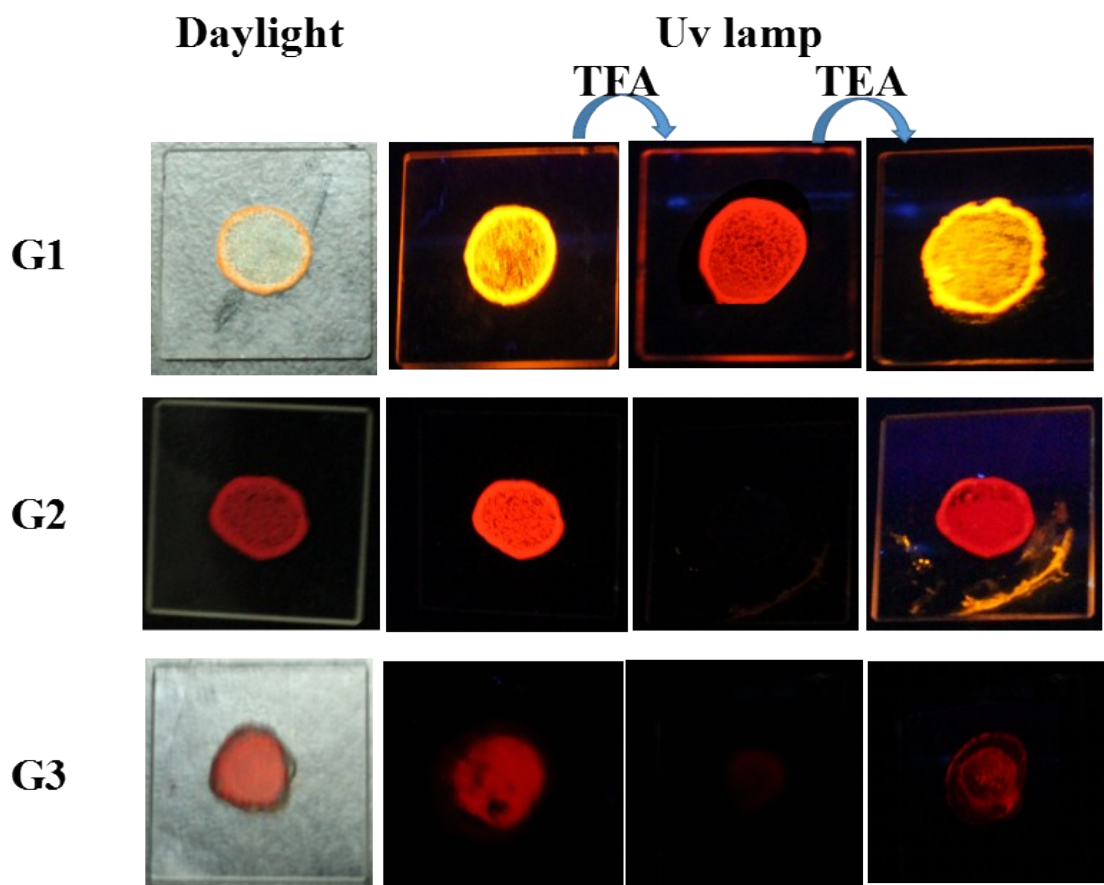


Fig. S12 Recycling of the fluorescence switching and color of **G1-G3** in solid state

upon fuming with TFA and TEA vapors under daylight (left) and 365 nm lamp (right)

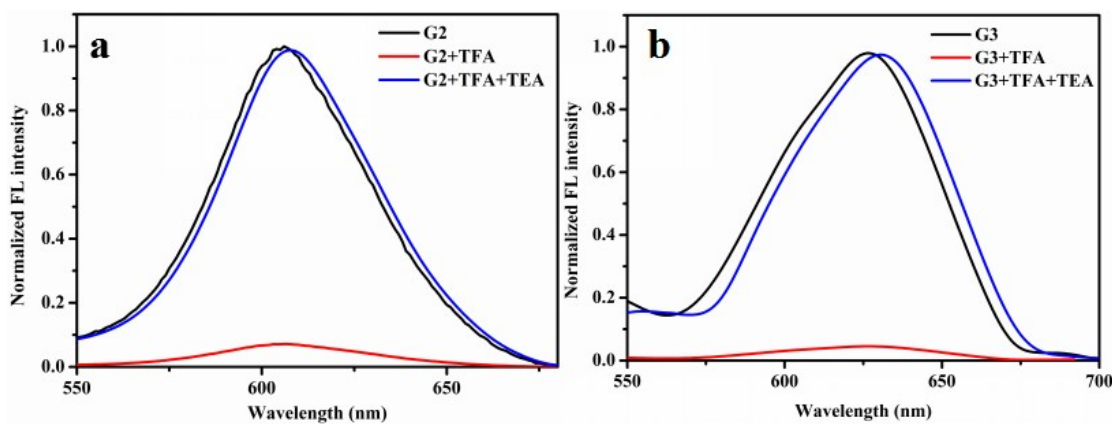


Fig. S13 The fluorescence spectra of **G2** and **G3** exposure to TFA and TEA vapors

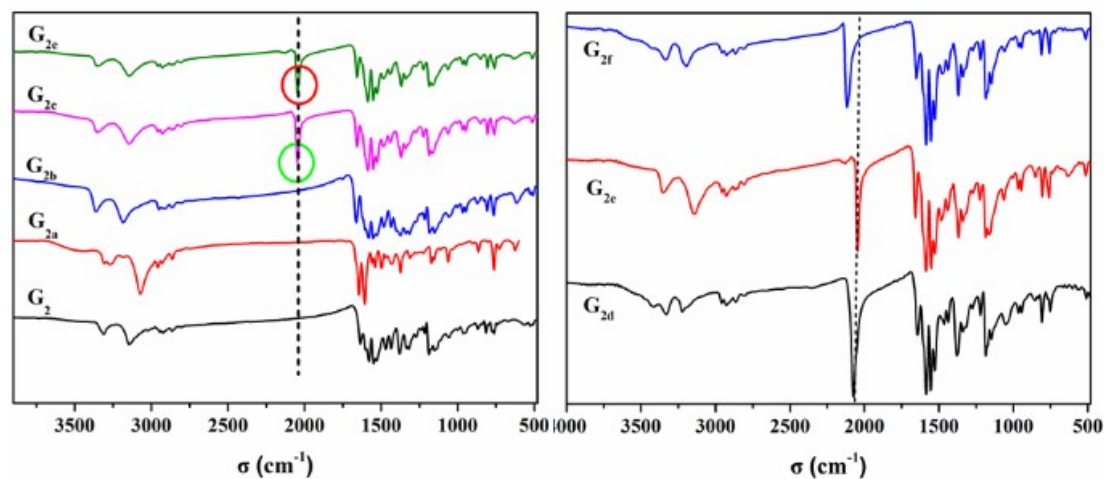


Fig. S14 FT-IR spectra of compounds **G_{2a}**-**G_{2f}** with different anions

Table S5 Emission wavelength of **G2** and **G_{2a}-G_{2f}**

Compounds	G2	G_{2a}	G_{2b}	G_{2c}	G_{2d}	G_{2e}	G_{2f}
-----------	-----------	-----------------------	-----------------------	-----------------------	-----------------------	-----------------------	-----------------------

Emission wavelengt (nm)	612	571	590	631	645	628	593
------------------------------------	-----	-----	-----	-----	-----	-----	-----

Table S6 Selected bond lengths (\AA) and angles ($^\circ$) of compound **G_{2b}**, **G_{2d}** and **G_{2f}**

	lengths (\AA)		angles ($^\circ$)
Compound G_{2b}			
C(19)-C(20)	1.408(3)	C(11)-N(3)-C(19)	120.35(15)
C(18)-C(23)	1.402(3)	C(19)-N(3)-C(13)	118.73(15)
C(18)-C(19)	1.409(3)	C(7)-C(8)-C(9)	123.93(18)
C(17)-N(2)	1.336(2)	C(23)-C(18)-C(17)	122.21(18)
C(3)-N(1)	1.360(3)	N(2)-C(17)-C(18)	121.79(17)
N(3)-C(13)	1.485(2)	N(1)-C(3)-C(4)	122.25(18)
N(3)-C(19)	1.395(2)	N(3)-C(11)-C(10)	120.46(17)
N(3)-C(11)	1.371(2)	N(3)-C(19)-C(18)	120.65(17)
N(4)-O(2)	1.209(2)	O(2)-N(4)-O(1)	119.13(18)

Compound G_{2d}

Zn(1)-N(5)	1.936(3)	N(5)-Zn(1)-N(5)	109.3(2)
Zn(1)-N(4)	1.965(3)	N(5)-Zn(1)-N(4)	108.30(13)
S(1)-C(24)	1.612(4)	N(5)-Zn(1)-N(4)	110.67(14)
S(2)-C(25)	1.610(4)	C(9)-N(2)-C(1)	120.7(2)
N(2)-C(9)	1.368(3)	C(1)-N(2)-C(20)	118.6(2)
N(2)-C(20)	1.509(4)	C(1)-C(6)-C(7)	118.7(3)
C(6)-C(1)	1.409(4)	N(1)-C(7)-C(8)	121.4(3)
C(7)-N(1)	1.346(4)	N(1)-C(7)-C(6)	z
C(17)-C(16)	1.368(4)	N(2)-C(1)-C(6)	120.0(3)
C(15)-C(14)	1.412(4)	C(9)-C(8)-H(8)	117(2)
S(1)-C(24)	1.612(4)	N(5)-Zn(1)-N(4)	110.67(14)

Compound G_{2f}

Hg(1)-S(3)	2.4364(18)	S(3)-Hg(1)-S(2)	137.86(6)
Hg(1)-S(2)	2.4547(17)	S(2)-Hg(1)-S(1)	111.83(6)
Hg(1)-S(1)	2.5297(19)	S(3)-Hg(1)-N(4)	93.39(16)
Hg(1)-N(4)	2.563(6)	S(1)-Hg(1)-N(4)	101.92(19)
S(2)-C(24)	1.648(8)	C(26)-S(3)-Hg(1)	97.7(3)
S(3)-C(26)	1.643(9)	N(4)-C(24)-S(2)	177.4(6)
N(6)-C(26)	1.130(10)	C(9)-N(2)-C(20)	120.3(4)
N(2)-C(9))	1.374(7)	N(2)-C(9)-C(8)	120.2(5)
N(2)-C(20)	1.482(7)	N(2)-C(4)-C(5)	120.9(5)

Table S7 Crystal data collections and structure refinements of compounds **G_{2b}**, **G_{2d}**
and **G_{2f}**

compounds	G_{2b}	G_{2d}	G_{2f}
empirical formula C	C ₂₃ H ₂₈ N ₄ O ₃	C ₅₀ H ₅₆ N ₁₀ S ₄ Zn	C ₂₆ H ₂₇ N ₆ S ₃ Hg
formula weight	408.49	990.66	720.31
crystal system	Monoclinic	Monoclinic	Triclinic
space group	P2 ₁ /n	C2/c	P-1
a [Å]	13.215(5)	20.941(5)	11.226(5)
b [Å]	10.327(5)	11.461(5)	11.535(5)
c [Å]	16.162(5)	22.337(5)	11.969(5)
α [°]	90.000(5)	90.000(5)	108.012(5)
β [°]	93.560(5)	107.490(5)	100.682(5)
γ [°]	90.000(5)	90.000(5)	90.099(5)
V [Å ³]	2201.4(15)	5113(3)	1445.5(11)
Z	4	4	2
T [K]	296(2)	296(2)	296(2)
D calcd [g·cm ⁻³]	1.233	1.287	1.655
μ [mm ⁻¹]	0.083	0.688	5.566

θ range [°]	2.34-24.84	2.34-20.32	2.33-23.02
total no. data	3870	4517	4711
no.unique data	2884	2736	3821
no.params refined	274	321	328
R_I	0.0471	0.0457	0.0308
wR_2	0.1356	0.1298	0.0834
Goodness-of-fit on F^2	1.001	0.999	0.997

Table S8 Hydrogen bond lengths (\AA) and bond angles ($^\circ$) of compounds **G_{2b}**, **G_{2d}** and **G_{2f}**

Compound G_{2b}				
D–H…A	<i>d</i> (D–H)	<i>d</i> (H…A)	<i>d</i> (D…A)	\angle DHA
C(7)–H(7)…N(4)	0.930	2.732	3.622	160.37
C(20)–H(20)…O(2)	0.930	2.622	3.454	149.22
C(15)–H(15B)…O(2)	0.970	2.557	3.407	146.40
C(13)–H(13B)…O(2)	0.970	2.455	3.296	144.90
C(13)–H(13B)…O(3)	0.970	2.692	3.611	158.29
N(2)–H(2B)…O(1)	0.860	2.054	2.831	149.83
C(9)–H(9)…O(3)	0.930	2.709	3.600	160.86
N(2)–H(2A)…O(1)	0.860	2.068	2.894	160.
C(23)–H(23)…O(2)	0.930	2.556	3.410	152.81
Compound G_{2d}				
D–H…A	<i>d</i> (D–H)	<i>d</i> (H…A)	<i>d</i> (D…A)	\angle DHA
C(5)–H(5)…N(1)	0.883	2.589	2.886	100.69
N(1)–H(1A)…N(4)	0.860	2.558	3.372	158.35
N(1)–H(1B)…S(2)	0.860	2.889	3.733	167.42
C(5)–H(5)…S(2)	0.883	2.923	3.738	154.27
C(3)–H(3)…N(4)	0.966	2.743	3.667	160.25
Compound G_{2f}				
D–H…A	<i>d</i> (D–H)	<i>d</i> (H…A)	<i>d</i> (D…A)	\angle DHA
C(5)–H(5)…N(4)	0.930	2.878	3.555	130.67
C(2)–H(2)…N(1)	0.930	2.613	2.902	98.61
N(1)–H(1A)…N(6)	0.860	2.428	3.238	157.25
N(1)–H(1B)…N(5)	0.860	2.132	2.969	164.25

C(2)–H(2)…N(5)	0.930	2.559	3.475	168.59
C(19)–H(19A)…N(1)	0.960	2.657	3.537	152.61

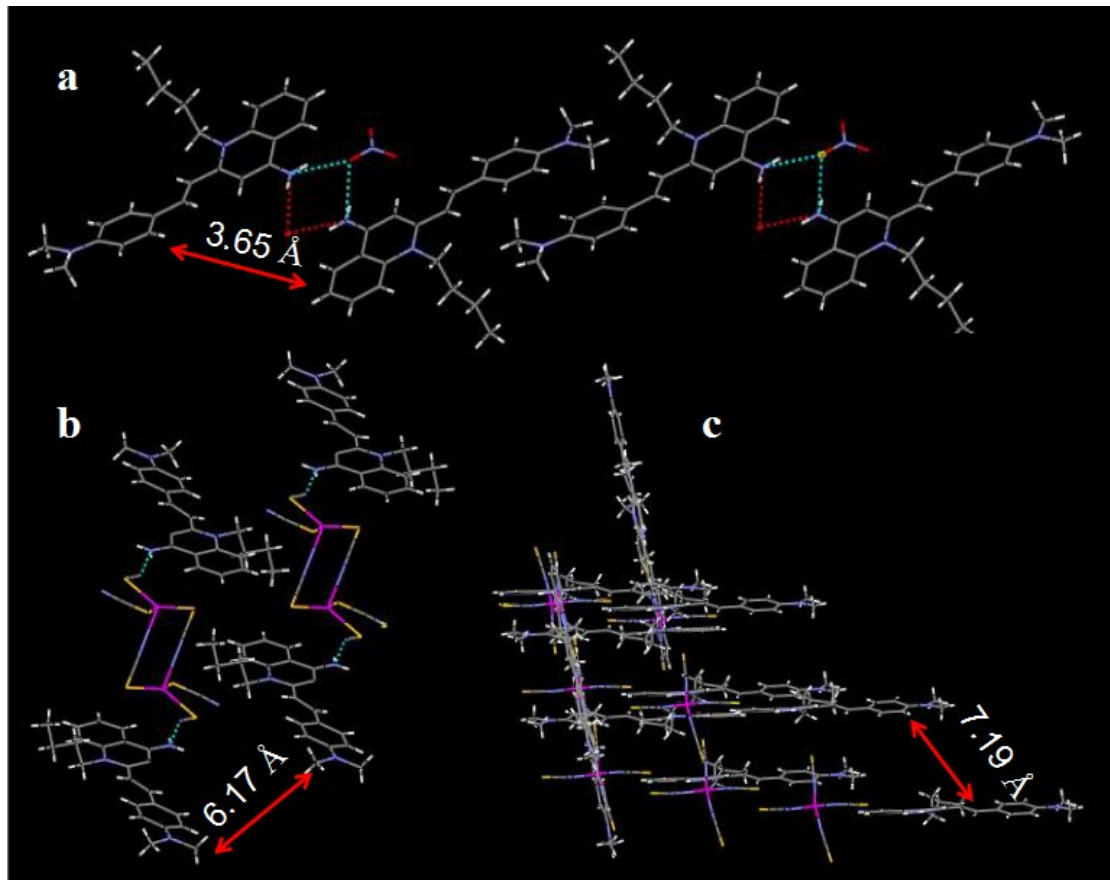


Fig. S15 Molecular arrangement of **G_{2b}** (a); **G_{2d}** (b) and **G_{2f}** (c).

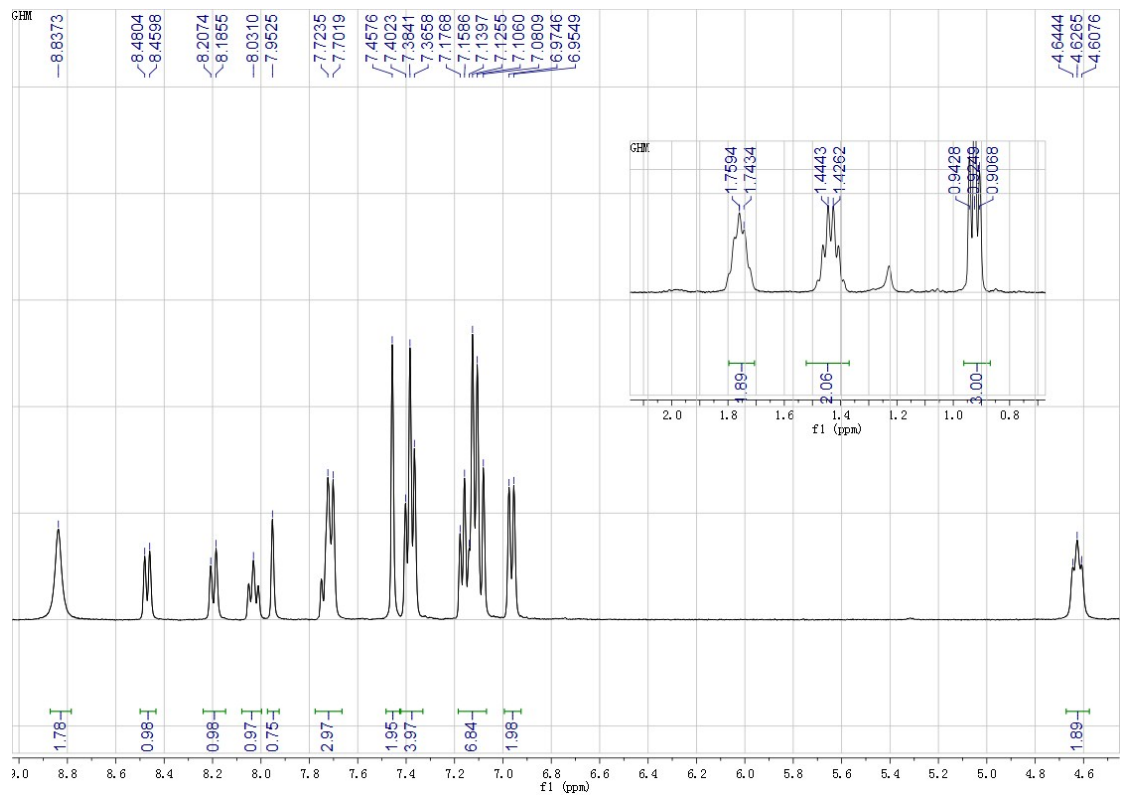


Fig. S16 ^1H NMR spectrum (400 MHz) of **G1** in $\text{DMSO}-d_6$

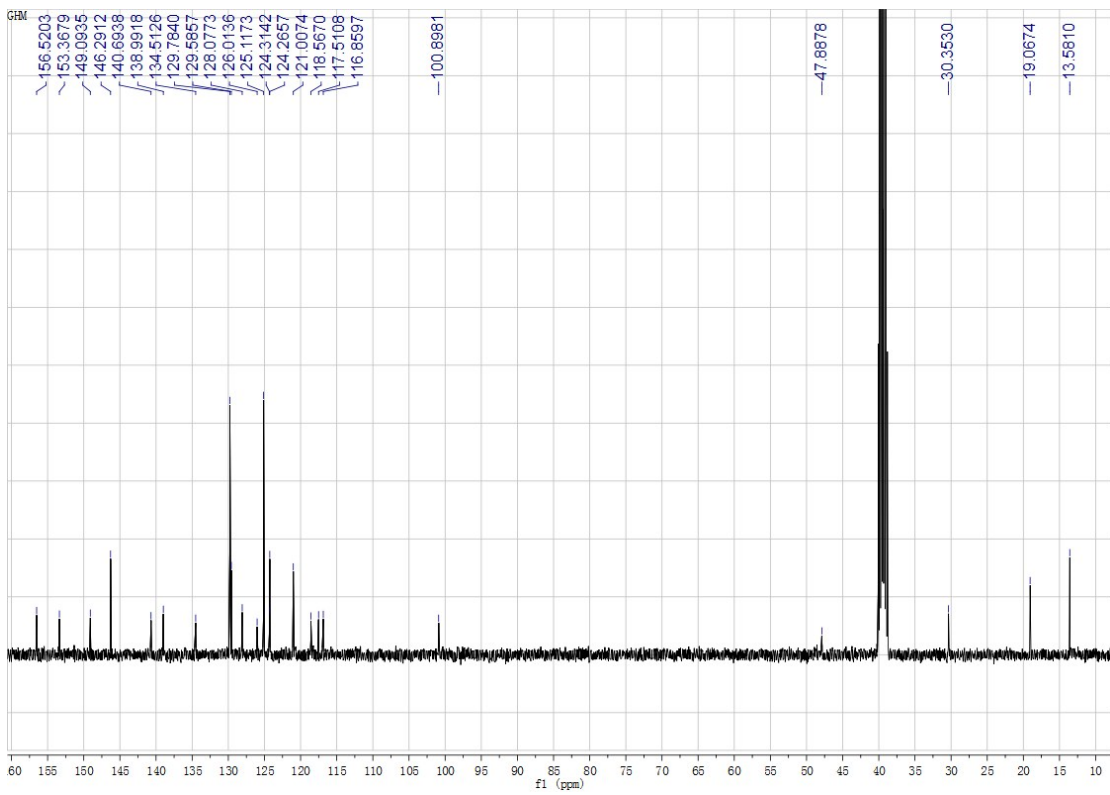


Fig. S17 ¹³C NMR spectrum (100 MHz) of **G1** in DMSO-*d*₆

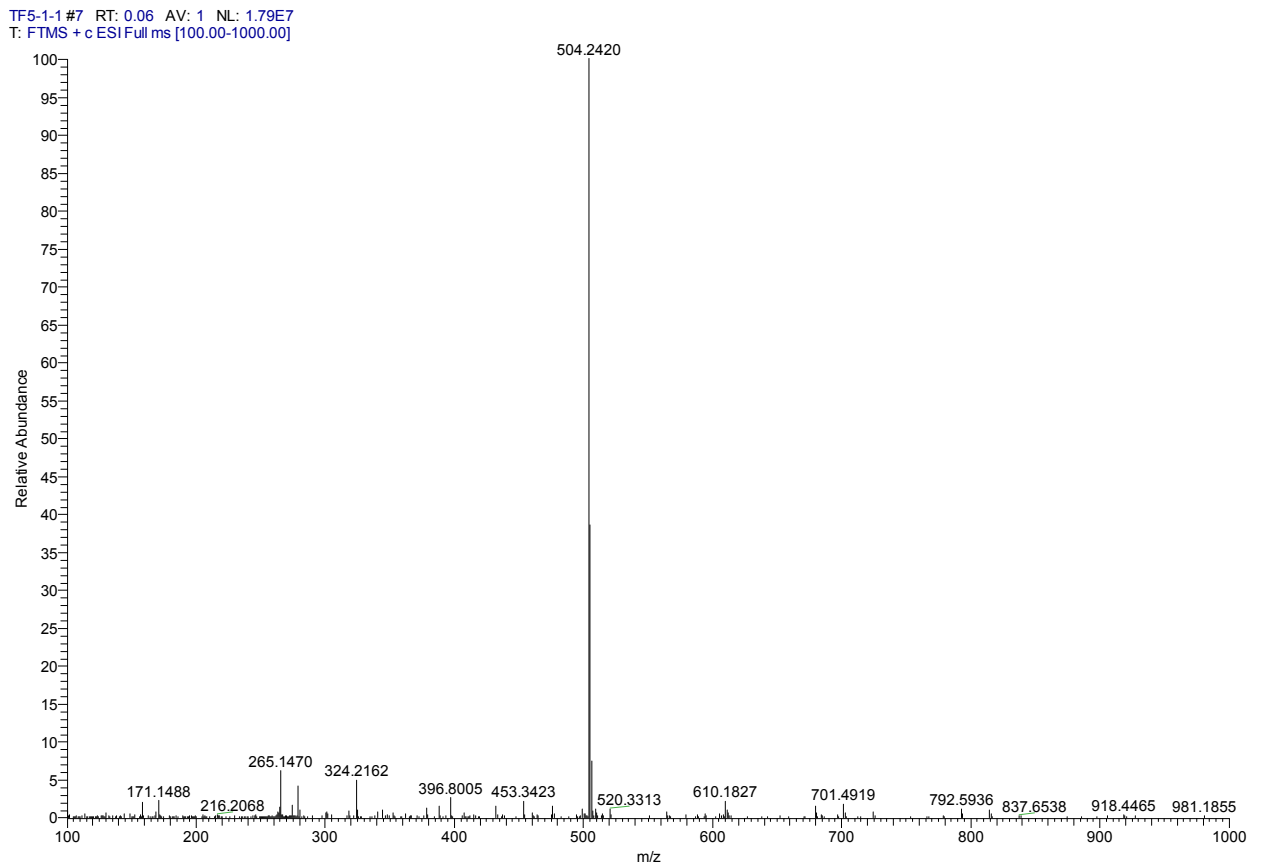


Fig. S18 ESI-MS spectrum of **G1**

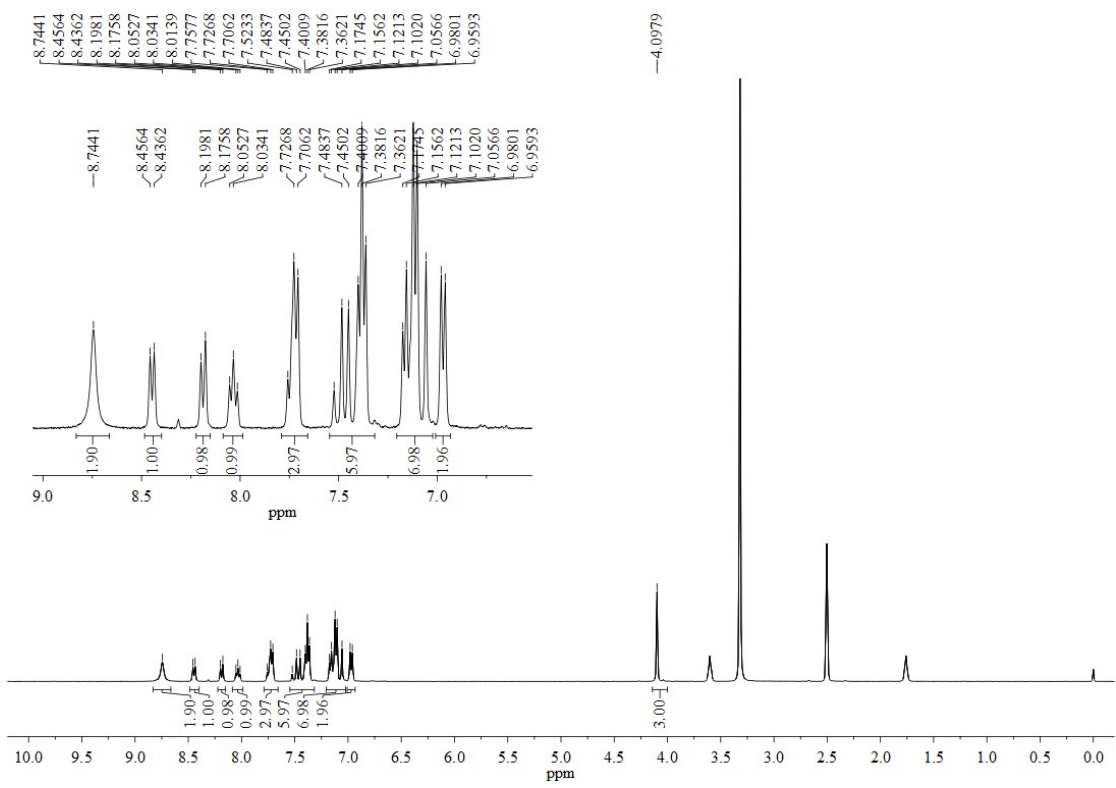


Fig. S19 ¹H NMR spectrum (400 MHz) of **G2** in $\text{DMSO}-d_6$

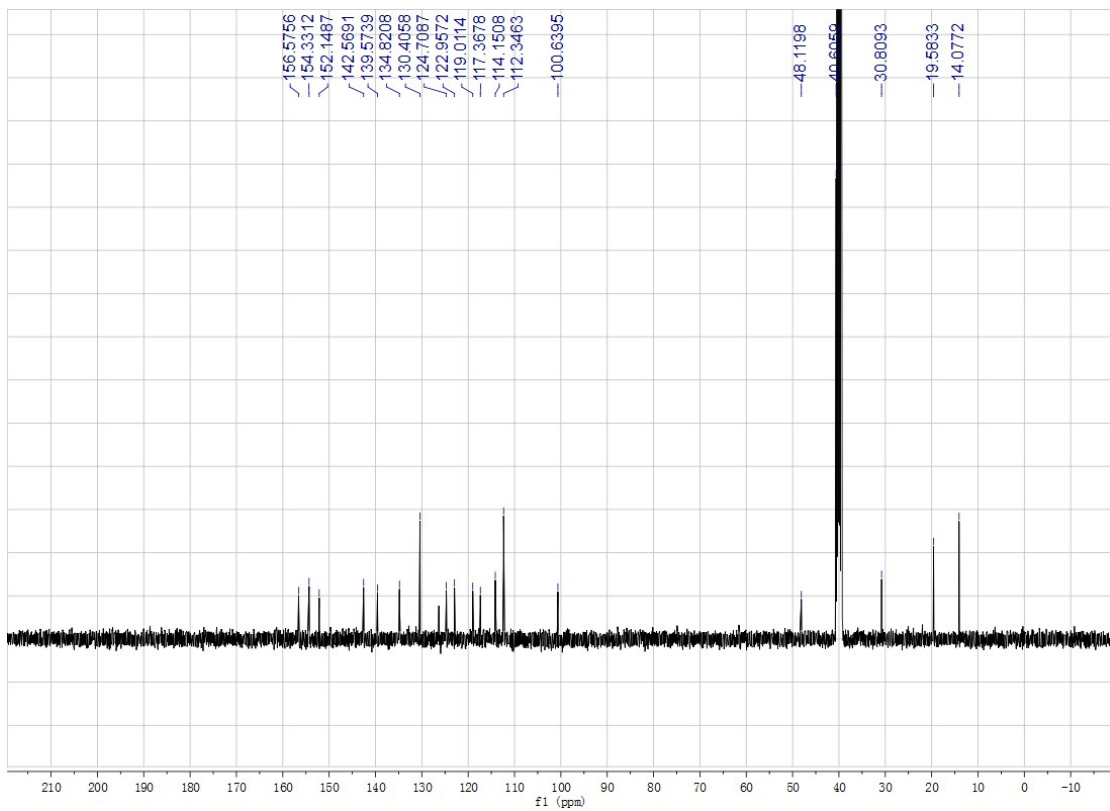


Fig. S20 ¹³C NMR spectrum (100 MHz) of **G1** DMSO-*d*₆

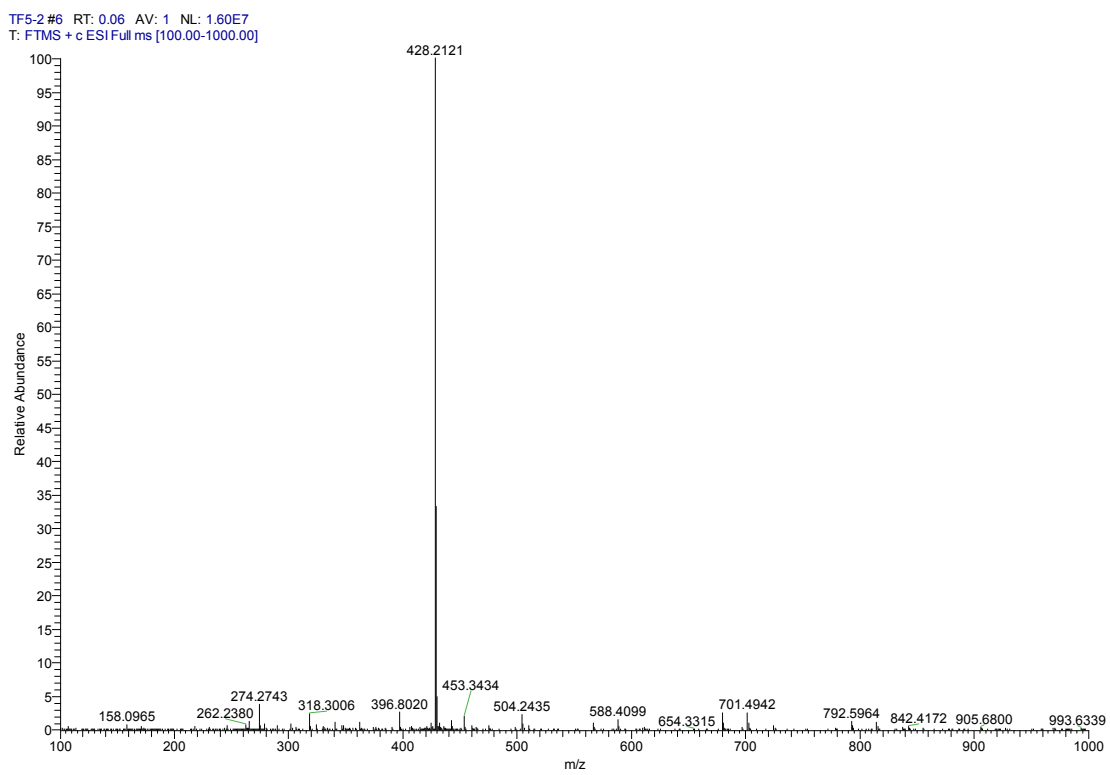


Fig. S21 ESI-MS spectrum of **G2**

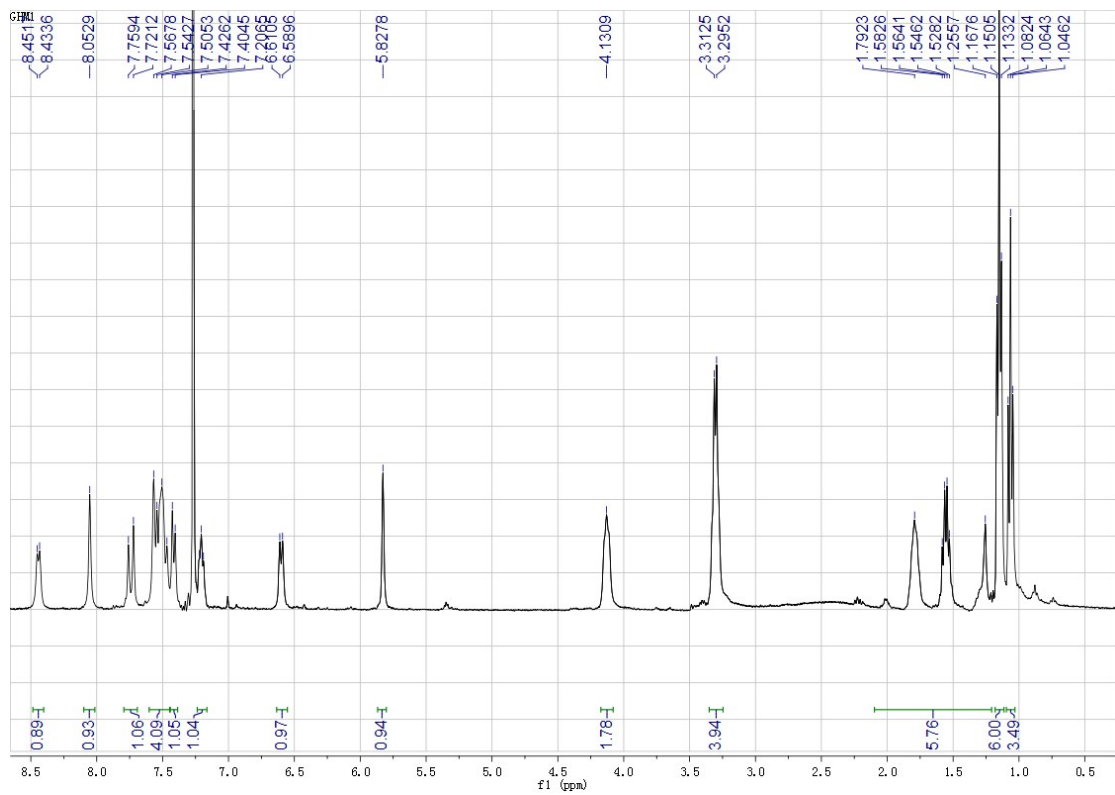


Fig. S22 ^1H NMR spectrum (400 MHz) of **G3** in CDCl_3

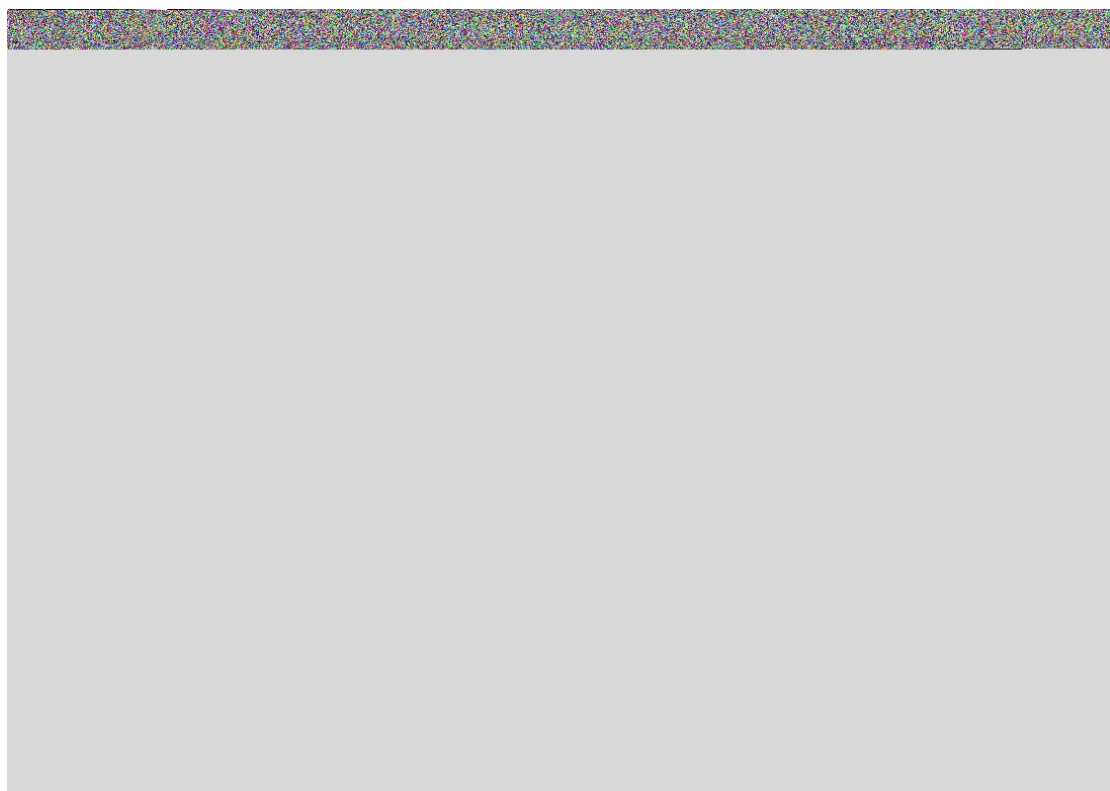


Fig. S23 ^{13}C NMR spectrum (100 MHz) of **G3** in CDCl_3

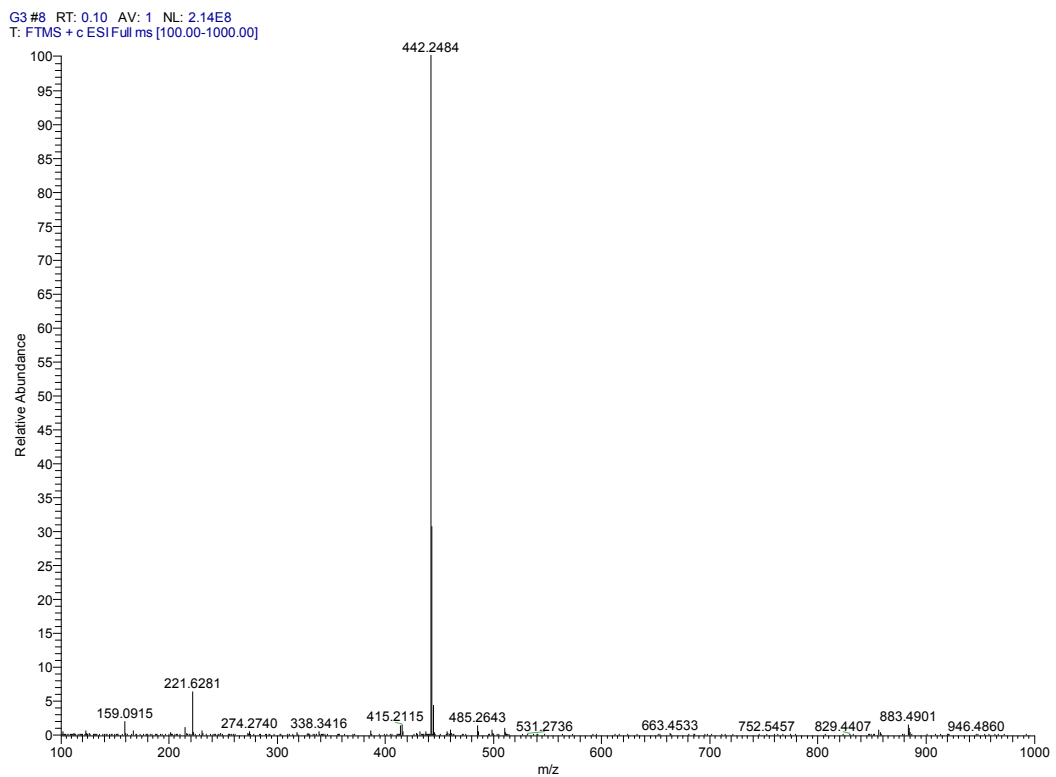


Fig. S24 ESI-MS spectrum of **G3**

